Journal of Applied Polymer Science

Mechanical Properties of Epoxy Resins Reinforced with Synthetic Boehmite (AlOOH) Nanosheets

Zhanjun Wu, Qin Zhuo, Tao Sun, Zhi Wang
School of Aeronautics and Astronautics, State Key Laboratory of Structural Analysis for Industrial Equipment, Dalian University of Technology, Dalian 116024, People's Republic of China
Correspondence to: T. Sun (E-mail: tsun@mail.dlut.edu.cn)

ABSTRACT: In this article, sheet boehmite (AlOOH), which was synthesized via a facile and environmental friendly method, was used as reinforcing agent to toughen Bisphenol A epoxy resin. The result of X–ray Diffraction (XRD) and IR spectrum indicated that the as–synthesized product was pure crystalline and high purity AlOOH. The effects of sheet AlOOH on the mechanical properties of AlOOH/epoxy nanocomposites were investigated. The results indicated that the introduction of AlOOH significantly improved the mechanical properties of epoxy resin. Compared with neat epoxy resin, the tensile strength and the fracture toughness (K_{IC}) of the AlOOH/epoxy nanocomposites filled with 4 wt % AlOOH increased by 24.2% and 28.7%, respectively, while the flexural strength increased from 40.92 to 50.00 MPa. From Scanning Electron Microscope (SEM), a phase-separated morphology and plenty of cervices and river branches were observed in the fractured surfaces of composites. With the increase of sheet AlOOH content, river-shaped cracks became more and more intensive. Overall, the addition of sheet AlOOH is shown as a promising method for mechanical properties enhancement of epoxy matrix. © 2014 Wiley Periodicals, Inc. J. Appl. Polym. Sci. **2015**, *132*, 41409.

KEYWORDS: mechanical properties; nanostructured polymers; resins

Received 12 May 2014; accepted 14 August 2014
DOI: 10.1002/app.41409

INTRODUCTION

Epoxy resin is noted for its outstanding properties such as good heat and chemical resistance, easy processability, low cost, high temperature performance, and low shrinkage on cure.[1–3] Because of its unique features, epoxy resin and its composites have wide applications in electrical insulators, coatings, aerospace, marine transportation and so on.[4–7] The resin forms a highly cross-linked network structure having relatively high stiffness, glass transition temperature (T_g) and high chemical resistance.[8] However, high crosslinking density may lead resins to be brittle, which affect the mechanical property and durability of the components. Therefore, plenty of researchers have done many excellent works in improving the toughness of epoxy resin. Among of them, forming epoxy composite by introduction of an appropriate toughening agent into epoxy matrix is the most common approach. The most common toughening agents include elastic rubber, thermoplastic resin, and polysiloxane.[9–13] For example, Abad groups[14] have studied the mechanical and thermal degradation behaviors of epoxy resin modified with a mixture of acrylonitrile–butadiene–styrene (ABS), the mechanical behavior was studied by tensile test and the results shown that the toughness improved when the test temperature increased. Thomas et al.[8] have reported that functionally terminated polybutadiene liquid rubber was incorporated into the epoxy resin matrix to improve the toughness of the resin. The fracture toughness and impact strength of modified epoxy improved, but the flexural strength and modulus of the modified samples were lower than that of the unmodified epoxy. However, as far as we know, the stiffness and other valuable performances of epoxy resins modified with elastic rubber and thermoplastic are significantly decreased.[15] Fortunately, inorganic nanoparticles can impart a number of desirable mechanical and barrier properties to the polymer owing to their unique mechanical and tribological properties, and high surface area to mass ratio et al. For example, Chen groups[16] have reported a route to synthesize epoxy nanocomposites filled with 12-nm spherical silica particles and investigated their mechanical properties. They found that the toughness and modulus of SiO_2/epoxy nanocomposites improved without sacrificing the working temperature of the resin. Naous groups[17] have investigated the mechanical properties of epoxy/Al_2O_3 nanocomposites, the results showed that storage modulus, Young's modulus and tensile strength of the epoxy improved with the incorporation of Al_2O_3 nanoparticles, increase in fracture toughness was also achieved for epoxy/Al_2O_3 nanocomposites with 2 vol % Al_2O_3, which indicated that the spherical Al_2O_3 nanoparticles had a significant influence for epoxy toughening without sacrificing

stiffness. As a second phase, the inorganic fillers can affect cure exotherms, shrinkage, thermal and electrical conductivity, machinability, hardness, compressive, flexural, and impact strength of composites.[18] Research results have showed that the microstructure and properties of composites, such as thermostability and rigidity, are affected by kinds, size, and shape of modifier particle.[19] AlOOH is an aluminum oxhydroxide which can be widely used precursor for preparation of many aluminum oxide materials. Nanoscale AlOOH is considered to be an additive, which could endow polymer materials with excellent mechanical properties due to its low cost, good chemical stability and high surface area.[20–22] And before then, the reports about the effects of AlOOH on the mechanical properties of epoxy resins are few in the open literatures.

In this work, the main purpose was to prepare a kind of epoxy composite with good mechanical properties. A facile and environment friendly route was firstly adopted to prepare sheet nano—AlOOH, which was used as toughening agent to toughen epoxy resin. The structure and morphology of the synthesized AlOOH and its effect on the mechanical properties of the formed AlOOH/epoxy nanocomposites were investigated in details.

EXPERIMENTAL

Materials

Bisphenol A epoxy resin (epoxy value is 0.51–0.53 mol/100 g) was purchased from Tianjin Ningping Chemical, China. Al $(NO_3)_3 \cdot 9H_2O$ and urea, analytically pure, were obtained from Tianjin Damao Chemical Reagent, China. 4,4′-diaminodiphenyl methane (DDM) was purchased from Sinopharm Chemical Reagent, China.

Experimental Procedures

In a typical synthesis procedure, 45.46 g of $Al(NO_3)_3 \cdot 9\ H_2O$ was first dissolved in 90 mL of water. After 13.65 g of urea was added, the mixture was stirring mildly at 50°C for 1 h. The obtained transparent solution was then transferred into a Teflon-lined autoclave of 150 mL and heated at 160°C for 24 h. After being cooled to room temperature naturally, the sample was filtered and washed with distilled water until its pH was neutral.

The AlOOH obtained above was dissolved in ethanol and mixed with 65.46 g bisphenol A epoxy resin dissolved in 20 mL acetone, the mixture was stirred at 90°C to eliminate ethanol and acetone in this solution. 24.81 g the curing agent (DDM) was added to the mixture, which was then put into a vacuum drying oven at 85°C for 30 min to eliminate air bubbles and residual acetone and ethanol, and then the mixture was added to the polytetrafluoroethylene mold and cured at 100°C for 2 h, 160°C for 4 h to get the AlOOH/epoxy nanocomposite samples. The mass percent of AlOOH in nanocomposite was set as 0, 1, 2, 3, and 4%, respectively.

Characterizations

The crystal structure was identified by the X–ray diffraction (XRD, Panalytical X'Pert Pro MPD, Netherlands, Cu Ka radiation, l = 1.54 A°). Fourier transform infrared (FTIR) spectrum for AlOOH was obtained using an EQUINOX55 FTIR spectrometer.

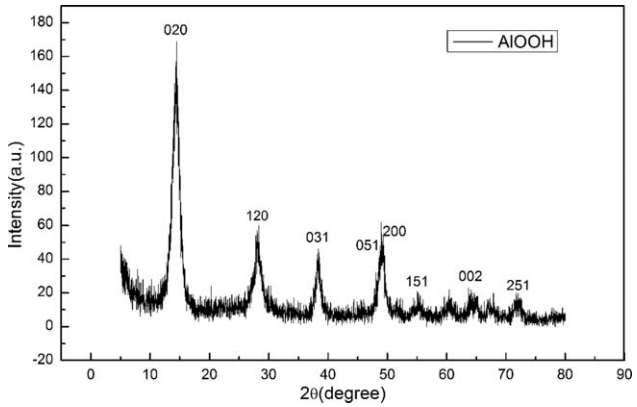

Figure 1. XRD spectrum of as-synthesized AlOOH.

Tensile properties were measured on an Instron testing machine (Model 3345 USA) at a testing rate of 1 mm/min according to the ASTM D 638. Bending tests were measured via a single–edge–notched (SEN) test as part of a three-point flexural test conducted using a universal test machine (Model 3345 USA) at a testing rate of 0.5 mm/min according to the ASTM D 790, the span to thickness ratio was 0.25. The values were taken from an average of five specimens.

Fractured surfaces of the specimens after tensile testing and structure analysis were performed at QUANTA 450. The fractured surfaces were coated with a thin layer of gold to improve conductivity before the observation by SEM. TEM was performed using a Tecnai G220 S-Twin transmission electron microscope.

RESULTS AND DISCUSSION

XRD Analysis

The crystalline phase of as-synthesized AlOOH was examined by XRD measurement. Figure 1 shows that the diffraction peaks of the as-prepared product can perfect in good agreement with the standard value of orthorhombic γ–AlOOH (JCPDSC 21–1307),[23] which indicate the as-prepared product is high purity AlOOH. The sharp peaks (020, 120, 031, and 200) indicate the obtained γ–AlOOH is high crystalline.

Morphological Characterization

Scanning electron microscope (SEM) and Transmission electron microscopy (TEM) was employed to investigate the morphology of the prepared AlOOH. From Figure 2(a), the thickness of the lamellar AlOOH sample is about 22.2 nm. Figure 2(b) shows that the prepared AlOOH has overlapped lamellar morphology and unambiguous boundaries between lamellar AlOOH samples can be distinguished. It indicates that the prepared lamellar AlOOH sample is independent and nonstick.

FTIR Analysis

To investigate purity of as-prepared AlOOH, the product was measured using an EQUINOX55 FTIR spectrometer, and the IR spectrum of the as-synthesized AlOOH is shown in Figure 3. As shown in the figure, all the absorption bands at 3392, 3099, 1635, 1157, 885, 752, 629, and 478 cm^{-1} are in good agreement with the values of those reported in the literatures, which prove that AlOOH is prepared. The strong, broad band at 3329 cm^{-1}

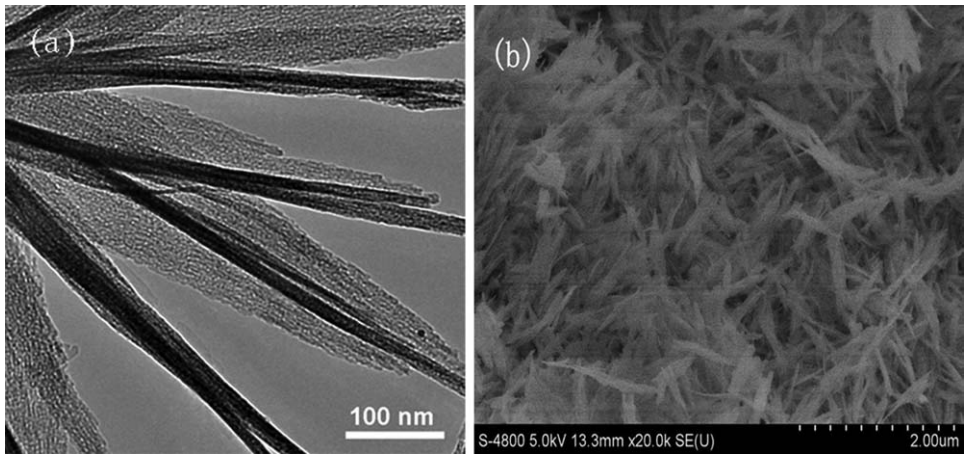

Figure 2. (a) TEM images of the synthesized AlOOH; (b) SEM micrograph of the synthesized AlOOH.

is assigned to stretching vibration of OH group in the hydroxide structure as well as in physically absorbed water,[24] and the intensive bands at 3099 cm^{-1} can be described to the υ_s (Al) O–H vibrations of AlOOH. The shoulder at 1639 cm^{-1} is taken for the bending mode of absorbed water. While the band at 1157 cm^{-1} is believed to be δ_{as} Al—O—H mode, the other bands located in 752, 629, 478 cm^{-1} belong to the AlO_6 vibration mode. No absorption bands from the other phase are observed in IR spectrum, which indicate the high purity of product.

Mechanical Behavior

Figure 4 shows the stress–strain curves of neat epoxy and AlOOH/epoxy nanocomposites. There is a noticeable increasing trend in the tensile strength of nanocomposites when the content of AlOOH is less than 2 wt %. When 2 wt % AlOOH was added, the tensile strength of the AlOOH/epoxy nanocomposites can increase from 62.92 to 82.71 MPa. As AlOOH content increases to 3 wt %, the tensile strength of the AlOOH/epoxy nanocomposites decreases slightly. However, the tensile strengths of nanocomposites are all higher than that of neat epoxy, which indicates that the AlOOH can exert its reinforcing effect on epoxy resins. The trends for the values of tensile modulus of unmodified epoxy and epoxy modified with AlOOH obtained from the stress–strain curves appear to be similar to those for the tensile strength vales. The stiffening effect induced by nanofiller incorporation is usually attributed to the formation of a rigid interphase between the matrix and the particles. Furthermore, as shown in Figure 4, the addition of AlOOH nanoparticles results in an enhancement of material ductility, producing an increase in strain at break of 55% for the 2 wt % AlOOH nanocomposites. Meanwhile, Figure 5(a) shows that the fractured surface after hand breaking of 2 wt % AlOOH nanocomposites has a big hole, which is not observed in the fractured surface after tensile test [Figure 5(b)]. The enhanced ductility can be explained by a failure mode in which particle debonding with massive voiding occurs first, followed by void coalescence associated with matrix fibrillation.[25]

The mechanical properties of the AlOOH/epoxy nanocomposites were further measured by a three-point bending test. The value of critical stress intensity factor (K_{IC}) is shown in Figure 6. K_{IC} are described by the state of stress in the vicinity of the tip of a crack as functions of the specimen geometry and the crack geometry.[26] K_{IC} was evaluated using single edge notch bending

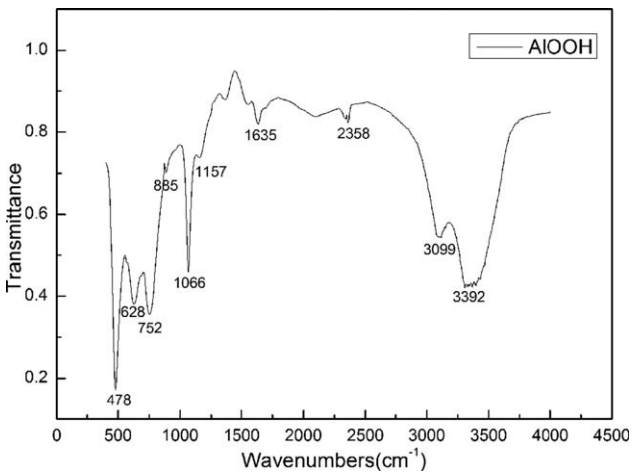

Figure 3. The FTIR spectra of the as-synthesized AlOOH.

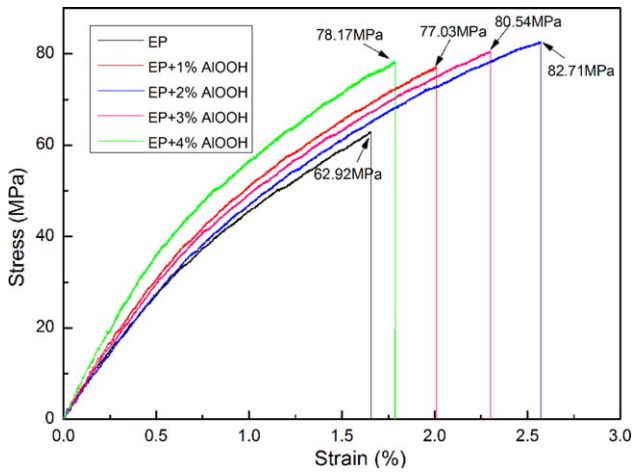

Figure 4. The stress–strain curves of pure epoxy and AlOOH/epoxy nanocomposites. [Color figure can be viewed in the online issue, which is available at wileyonlinelibrary.com.]

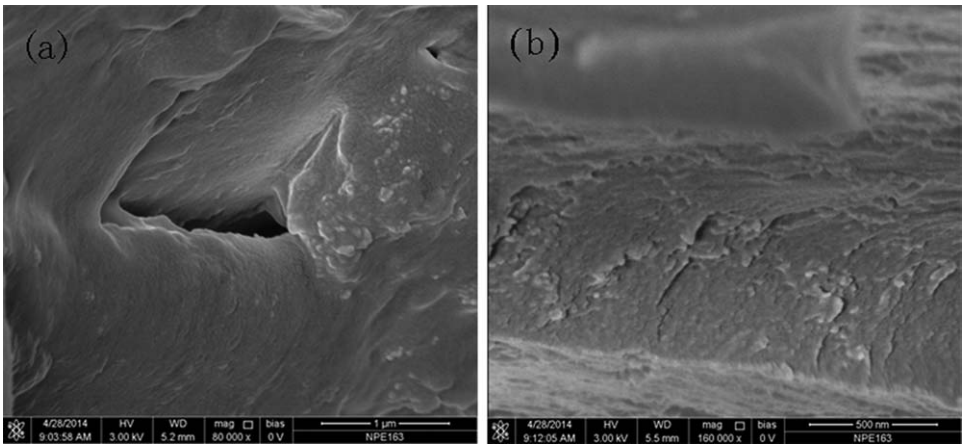

Figure 5. SEM images of the fractured surfaces of epoxy+2 wt % AlOOH: (a) after hand breaking; (b) after tensile test.

(SENB) specimens. A notch was introduced at the central of the specimen bar using a diamond blade saw followed by introducing sharp pre-crack into the notch via tapping a sharp razor blade. The ratio of notch length to width (a/w) was about 0.4. Fracture toughness (K_{IC}) was calculated using the following equation according to[27]

$$K_{IC} = \frac{P_m S}{WD^{\frac{3}{2}}} f\left(\frac{a}{w}\right)$$

where P_m is the maximum load at crack extension, S is the span of the sample, D is the specimen thickness, and W is the specimen width, a is the crack length, and $f\ (a/w)$ is the polynomial geometrical correction factor give as

$$f\left(\frac{a}{w}\right) = \frac{3\left(\frac{a}{w}\right)^{\frac{1}{2}}\left[1.99-\left(\frac{a}{w}\right)\left(1-\frac{a}{w}\right)\times\left(2.15-\frac{3.93a}{w}+2.7\frac{a^2}{w^2}\right)\right]}{2\left(1+\frac{2a}{w}\right)\left(1-\frac{a}{w}\right)^{\frac{3}{2}}}$$

From Figure 6, the K_{IC} value of neat epoxy is 3.07 MPa·m$^{1/2}$. After adding 2 wt % AlOOH, the K_{IC} value of the epoxy can increase by 27.8% (from 3.07 to 3.83 MPa·m$^{1/2}$). As the AlOOH content further increases to 3 wt %, the toughness of nanocomposites increases slightly. Anyway, adding 4 wt % AlOOH nanoparticles into the epoxy resin, the K_{IC} value of the nanocomposites can reach to 3.95 MPa m$^{1/2}$, which is about 0.88 MPa m$^{1/2}$ higher than that of neat epoxy. In particular, this value is higher than literature value which was reported by Jin et al.[15] The flexural strength of AlOOH/ epoxy nanocomposites is shown in Figure 7. The value was calculated by following equation:[28]

$$\sigma_f = \frac{3P_m S}{2WD^2}$$

where P_m is the rupture force (in N), S is the span of the sample (in mm), W is the specimen width (in mm), D is the specimen thickness (in m). As shown in Figure 7, one can know that the flexural strength of AlOOH/ epoxy composites containing 1 wt % AlOOH increases by 16.1% in comparison to unmodified epoxy system. The flexural strength filled with 2, 3, and 4 wt % is 47.84, 48.48, and 50.0 MPa, respectively. Clearly, with the increase of added AlOOH, the flexural strength of the nanocomposites shows no significant change. The low content AlOOH may have good dispersion in the epoxy matrix, when the content of AlOOH particle exceeds 2 wt %, the particle will reunite, homogeneous dispersion may prompt a perfect interfacial bonding between the AlOOH and epoxy matrix that facilitates load transfer.

Table I presents the whole results of tensile and flexural tests. Clearly, the tensile strength and fracture toughness can be

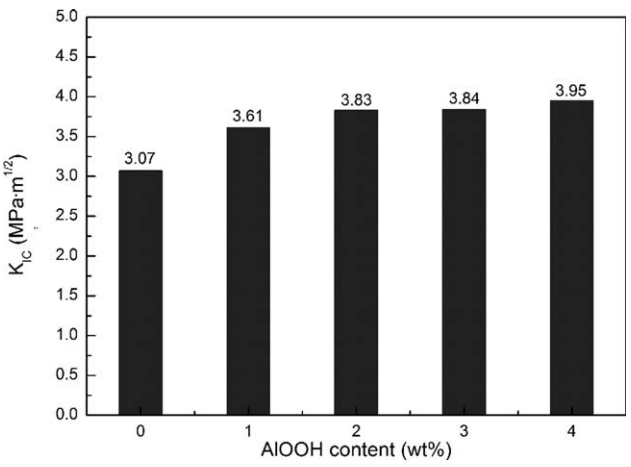

Figure 6. K_{IC} values of AlOOH/epoxy nanocomposites.

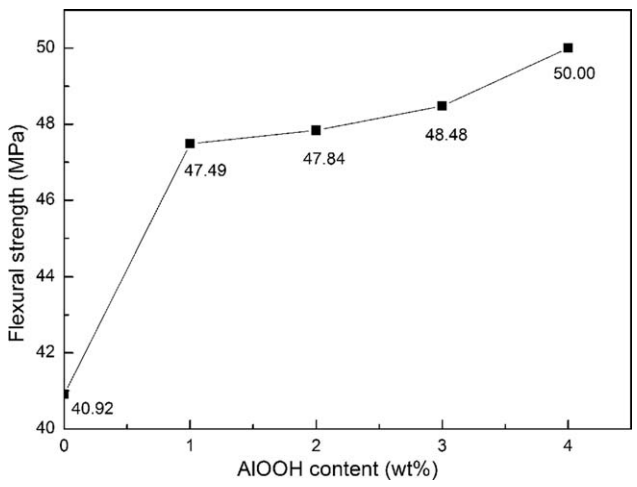

Figure 7. Flexural strength of AlOOH/epoxy nanocomposites.

Table I. Flexural and Tensile Properties of AlOOH/Epoxy Composites

AlOOH content (wt %)	Tensile strength (MPa)	K_{IC} (MPa $m^{1/2}$)	Flexural strength (MPa)
0	62.92	3.07	40.92
1	77.03	3.61	47.49
2	82.71	3.83	47.84
3	80.54	3.84	48.48
4	78.17	3.95	50.00

simultaneously improved by the addition of AlOOH with appropriate content. The hydroxyl of AlOOH nanoparticles can covalently bonded with resins which contain reactive groups, such as hydroxyl. The epoxide ring of epoxy resin is also one of the reactive groups. Epoxy resin and AlOOH will be covalent bonded together. Exner groups[29] have demonstrated that the epoxy ring reacts directly with the hydroxyl group of the boehmite (AlOOH) surface, the equation between the epoxy and AlOOH as shown in Scheme 1. The covalent bonding between the resin and AlOOH filler allows better load-transfer of mechanical loads to nanoparticles and also improves the toughness of AlOOH/epoxy nanocomposites since numerous bonds must be broken before cracks can propagate through the resin.[18]

Fractography

The morphologies of the AlOOH/epoxy nanocomposites were examined by SEM. The fractured surfaces of neat and modified epoxies are shown in Figure 8. The fractured surfaces of the neat epoxy resin after tensile test [Figure 8(a)] shows an

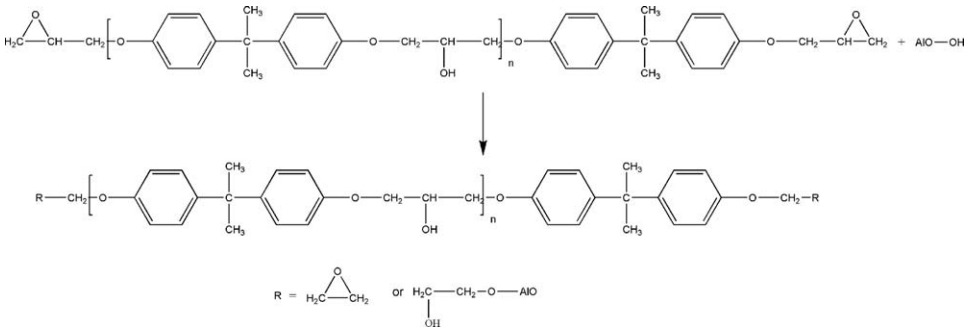

Scheme 1. Equation between the epoxy and AlOOH.

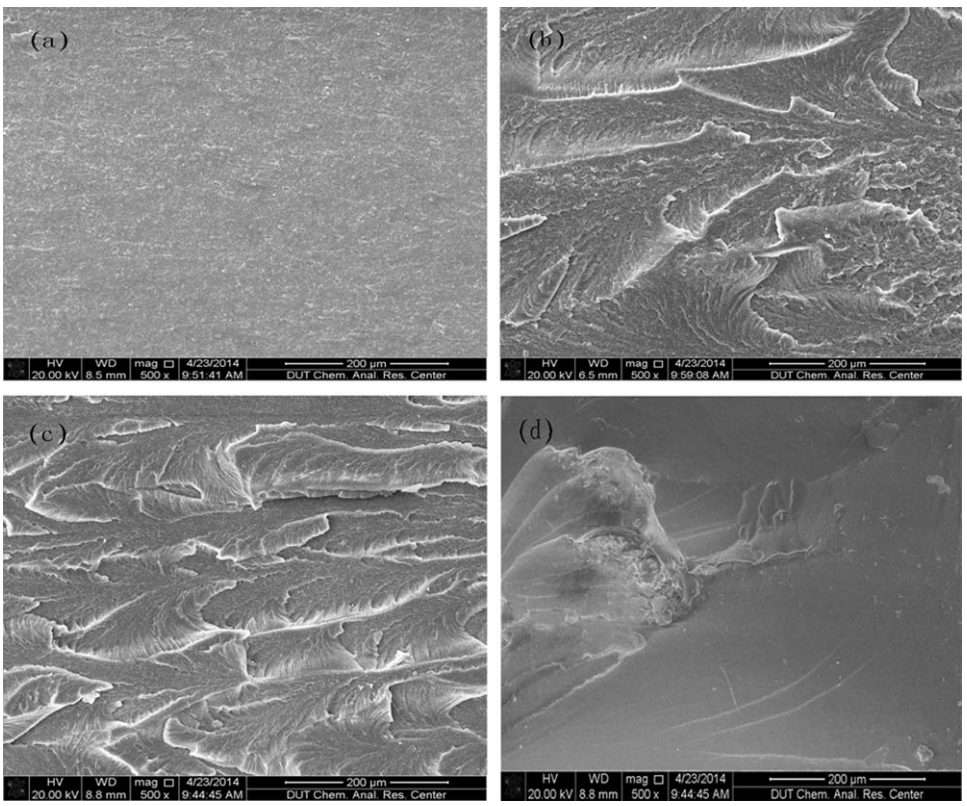

Figure 8. The fractured surfaces of unmodified and AlOOH-modified epoxy resins: (a) neat epoxy; (b) epoxy+1 wt % AlOOH; (c) epoxy+2 wt % AlOOH; (d) epoxy + 4 wt % AlOOH.

obviously smooth surface and the cracks spread freely and irregularly, which are the typical symbol of brittle fracture behavior.[30] Unlike the neat epoxy showing a smooth fractured surface, the AlOOH/epoxy nanocomposites present very rough failure morphologies. Plenty of crevices and river branches are observed in Figure 8(b,c), furthermore, as the increasing of the content of AlOOH, river-shaped cracks become more and more intensive. This river branches, which caused by load transferring from brittle epoxy resin to covalent bonding rigid AlOOH, are observed in the fracture of epoxy composite and are absent in that of neat epoxy resin. Good dispersion of AlOOH will lead to uniform fracture surface equally distributed river-shaped branches. Otherwise, the opposite is the case. From Figure 8(d), as the mechanical properties of the above analysis, the content of AlOOH particle in the resins exceeds 2 wt %, the particle will reunite. When cracks occur, the filler AlOOH might be viewed as stress concentrators to alter the direction of crack extension, thus making for the decrease of external energy. Therefore, adding AlOOH nanoparticles to matrixes can improve the fracture toughness of epoxy resin.

CONCLUSIONS

This work presents the characterization of a system of AlOOH/epoxy nanocomposites, which shows that the tensile strength and fracture toughness of the resin can be simultaneously improved. The analysis results of the XRD indicate that as-synthesized AlOOH is high pure and crystalline γ–AlOOH. The tensile tests of neat epoxy resin and AlOOH/epoxy nanocomposites with different content of AlOOH (1, 2, 3, and 4 wt %, respectively) indicate that tensile strength of AlOOH/epoxy nanocomposites are all higher than that of pure epoxy. The highest tensile strength is obtained when the loading of the AlOOH is 2 wt % (82.71 MPa). Both the flexural strength and fracture toughness (K_{IC}) are increased with the increase of the loading of the AlOOH. The flexural strength of composites filled with 4 wt % is 50.00 MPa, which is 9.08 MPa higher than that of neat epoxy. The fracture toughness (K_{IC}) of the epoxy composite containing 4 wt % AlOOH can increase by 28.7% (from 3.07 to 3.95 MPa $m^{1/2}$). The fractured surfaces of AlOOH/epoxy nanocomposites present a phase-separated morphology and plenty of cervices and river branches. These results indicate that sheet nano-AlOOH is effective reinforcing agents for epoxy resin. Because of the improved mechanical properties, this approach appears promising for use in the manufacturing of advanced reinforced composites.

ACKNOWLEDGMENTS

This work was supported by Fundamental Research Funds for the Central Universities (DUT10ZDG05) and the National Natural Science Foundation of China (51102031, 51002019, and 91016024).

REFERENCES

1. Huang, X. B.; Wei, W.; Wei, H.; Li, Y. H.; Gu, X. J.; Tang, X. Z. *J. Appl. Polym. Sci.* **2013**, *130*, 248.
2. Liu, Y.; Wu, W.; Chen, Y.; Shi, P. P.; Liu, M. C.; Wu, X. *J. Appl. Polym. Sci.* **2013**, *127*, 3213.
3. Reiko, S.; Yosuke, F.; Tohru, K. *J. Appl. Polym. Sci.* **2013**, *127*, 2074.
4. Chen, K.; Tian, C.; Lu, A.; Zhou, Q.; Jia, X.; Wang, J. *J. Appl. Polym. Sci.* **2014**, *131*, doi: 10.1002/app.40068.
5. Hesami, M.; Bagheri, R.; Masoomi, M. *J. Appl. Polym. Sci.* **2014**, *131*, doi: 10.1002/app.39849.
6. Du, K.; Yang, G.; Yuan, Z.; Xu, W.; Liang, X. *J. Appl. Polym. Sci.* **2014**, *131*, doi: 10.1002/app.40051.
7. Nogueira, P.; Ramirez, C.; Torres, A.; Abad, M. J.; Cano, J.; Lopez, J.; Lopez-Bueno, I.; Barral, L. *J. Appl. Polym. Sci.* **2001**, *80*, 71.
8. Thomas, R.; Yumei, D.; Yuelong, H.; Le, Y.; Moldenaers, P.; Weimin, Y.; Czigany, T.; Thomas, S. *Polymers* **2008**, *49*, 278.
9. Rosso, P.; Ye, L.; Friedrich, K.; Sprenger, S. *J. Appl. Polym. Sci.* **2006**, *100*, 1849.
10. Dinakaran, K.; Alagar, M.; Suresh Kumar, R. *Eur. Polym. J.* **2003**, *39*, 2225.
11. Nigam, V.; Setua, D. K.; Mathur, G. N. *J. Appl. Polym. Sci.* **2003**, *87*, 861.
12. Thomas, R.; Abraham, J.; Thomas, P.; Thomas, S. *J. Polym. Sci. Part B: Polym. Phys.* **2004**, *42*, 2531.
13. Chikhi, N.; Fellahi, S.; Bakar, M. *Eur. Polym. J.* **2002**, *38*, 251.
14. Abad, M. J.; Barral, L.; Cano, J.; Lopez, J.; Nogueira, P.; Ramírez, C.; Torres, A. *Eur. Polym. J.* **2001**, *37*, 1613.
15. Jin, F. L.; Park, S. *J. Polym. Degrad. Stab.* **2007**, *92*, 509.
16. Chen, C.; Justice, R. S.; Schaefer, D. W.; Baur, J. W. *Polymers* **2008**, *49*, 3805.
17. Naous, W.; Yu, X. Y.; Zhang, Q. X.; Naito, K.; Kagawa, Y. *J. Polym. Sci. Part B: Polym. Phys.* **2006**, *44*, 1466.
18. Shahid, N.; Villate, R. G.; Barron, A. R. *Compos. Sci. Technol.* **2005**, *65*, 2250.
19. Wang, H.; Han, W.; Tian, H.; Wang, Y. *Mater. Lett.* **2005**, *59*, 94.
20. Corcione, C. E.; Cataldi, A.; Frigione, M. *J. Appl. Polym. Sci.* **2013**, *128*, 4102.
21. Bravet, D.; Guiselin, O.; Swei, G. *J. Appl. Polym. Sci.* **2010**, *116*, 373.
22. Li, G.; Liu, Y.; Liu, D.; Liu, L.; Liu, C. *Mater. Res. Bull.* **2010**, *45*, 1487.
23. Tang, Z.; Liang, J.; Li, X.; Li, J.; Guo, H.; Liu, Y.; Liu, C. *J. Solid State Chem.* **2013**, *202*, 305.
24. Alemi, A.; Hosseinpour, Z.; Dolatyari, M.; Bakhtiari, A. *Phys. Status Solidi B* **2012**, *249*, 1264.
25. Pedrazzoli, D.; Khumalo, V. M.; Karger-Kocsis, J.; Pegoretti, A. *Polym. Test.* **2014**, *35*, 92.
26. Kim, B. J.; Bae, K. M.; Seo, M. K.; An, K. H.; Park, S. *J. Mater. Sci. Eng. A* **2011**, *528*, 4953.
27. Alamri, H.; Low, I. M. *Mater. Des.* **2012**, *42*, 214.
28. Jin, F. L.; Ma, C. J.; Park, S. *J. Mater. Sci. Eng. A* **2011**, *528*, 8517.
29. Exner, W.; Arlt, C.; Mahrholz, T.; Riedel, U.; Sinapius, M. *Compos. Sci. Technol.* **2012**, *72*, 1153.
30. Chen, Z. K.; Yang, G.; Yang, J. P.; Fu, S. Y.; Ye, L.; Huang, Y. G. *Polymer* **2009**, *50*, 1316.